TISSUE ENGINEERING: Part A
Volume 19, Numbers 17 and 18, 2013

DOI: 10.1089/ten.tea.2012.0605

Enhancement of Renal Epithelial Cell Functions through Microfluidic-Based Coculture with Adipose-Derived Stem Cells

Hui-Chun Huang, MS,[1,2] Ya-Ju Chang, MS,[1,2] Wan-Chun Chen, MS,[2,3] Hans I-Chen Harn, MS,[2,3] Ming-Jer Tang, MD, PhD,[2,3] and Chia-Ching Wu, PhD[1,2,4,5]

Current hemodialysis has functional limitations and is insufficient for renal transplantation. The bioartificial tubule device has been developed to contribute to metabolic functions by implanting renal epithelial cells into hollow tubes and showed a higher survival rate in acute kidney injury patients. In healthy kidney, epithelial cells are surrounded by various types of cells that interact with extracellular matrices, which are primarily composed of laminin and collagen. The current study developed a microfluidic coculture platform to enhance epithelial cell function in bioartificial microenvironments with multiple microfluidic channels that are microfabricated by polydimethylsiloxane. Collagen gel (CG) encapsulated with adipose-derived stem cells (CG-ASC) was injected into a central microfluidic channel for three-dimensional (3D) culture. The resuspended Madin-Darby canine kidney (MDCK) cells were injected into nascent channels and formed an epithelial monolayer. In comparison to coculture different cells using the commercial transwell system, the current coculture device allowed living cell monitoring of both the MDCK epithelial monolayer and CG-ASC in a 3D microenvironment. By coculture with CG-ASC, the cell height was increased with columnar shapes in MDCK. Promotion of cilia formation and functional expression of the ion transport protein in MDCK were also observed in the cocultured microfluidic device. When applying fluid flow, the intracellular protein dynamics can be monitored in the current platform by using the time-lapse confocal microscopy and transfection of GFP-tubulin plasmid in MDCK. Thus, this microfluidic coculture device provides the renal epithelial cells with both morphological and functional improvements that may avail to develop bioartificial renal chips.

Introduction

This article describes the functionalization of kidney epithelial cells with capsule-like constitution in a coculture microfluidic device. Microfluidic-based approaches have expensively been developed with the innovations in the Bio-Micro-Electro-Mechanical System (BioMEMS).[1] To date, several pieces of literature have reported to probe biological/physiological-relevant issues (e.g., cell–cell interactions, cell migration, cancer angiogenesis, and drug testing) through microfluidics with various engineering designs.[2,3] Using BioMEMS techniques to create a well-confined biological microenvironment for various types of mammalian cells, the coculture system can be achieved with a two-dimensional (2D) format by micropatterning a thin layer of the extracellular matrix (ECM)[4–6] or in a three-dimensional (3D) microfabricated matrix.[7] Both 2D and 3D platforms can be used to monitor the living cells for studying intracellular responses during the cell–cell interactions, which is a procedure superior to regularly mixing cultures and the transwell filter insert coculture systems. The coculture devices made via BioMEMS techniques can also allow us to understand direct the cell–cell contact between different types of cells. Some microfluidic devices were recently developed to reconstitute the tissue arrangements by coculturing the living cells within the features observed in living organs (for review, please see Ref.[8]). The concepts of "organs-on-chips" or "microtissue-on-chip" were proposed to study the physiology in an organ-specific context, develop specialized *in vitro* disease models, and analyze the transcriptomic and proteomic functional profiles.[8,9]

In kidney failure, the therapeutic strategies of renal replacement are still more sufficient than those of current hemodialysis.[10] Although hemodialysis can remove the end metabolites and correct the acid base and electrolyte abnormalities by intermittent diffusive processes, the functional limitations are due to the loss in tubular metabolic and endocrine secretions. The bioartificial tubule device (BTD),

[1]Department of Cell Biology and Anatomy, [2]Institute of Basic Medical Science, [3]Department of Physiology, [4]Department of Biomedical Engineering, and [5]Medical Device Innovation Center, National Cheng Kung University, Tainan, Taiwan.

incorporates the proximal tubular epithelial cells of the kidney, and is considered to play a vital role in treating acute kidney injury and chronic renal failure by contributing to the metabolic function and preventing inflammatory responses.[11] The basic BTDs were developed in several types of renal tubular cells to examine their interactions with the ECM and artificial membranes,[11] or the metabolic function of renal cell devices.[12,13] The BTD removed inflammatory cytokines *in vitro* and could be utilized for treatment of acute uremic animals.[10] However, the overgrowth of cells and multilayer formation in long-term cultures consequently limited the application of BTD.

The functional renal epithelial cell with maintenance of a confluent monolayer plays an important role in renal homeostasis.[14–16] The adipose tissue has recently been shown to be involved in the pathophysiology of renal disease and kidney failure.[17] Previous studies have demonstrated that the adipose tissue can allow Madin-Darby canine kidney (MDCK) epithelial cells to develop a tall columnar shape with increased production of glycogen and to increase the size of MDCK cells in their coculture.[18] Adipose-derived stem cells (ASCs) are confirmed as a source of multipotent stem cells that can be differentiated into osteogenic, chondrogenic, myogenic, and adipogenic cells in the presence of lineage-specific induction factors *in vitro*.[19,20] In the family of mesenchymal stem cells (MSCs), the ASCs possess similar characteristics of multipotency, molecular signatures, and share common genetic signals similar to those of bone marrow MSCs (BM-MSCs).[21,22] Hence, the current study is interested in developing a microfluidic device to improve renal function in epithelial cells by coculture with ASCs. In this coculture system, the two types of cells were cultured inside microfluidic channels individually.

We aim to utilize BioMEMS techniques to create a coculture system with a combination of living cell microscopy and the application of fluidic shear stress. The feature of Bowman's capsule in the nephron was manufactured for the proposed coculture microfluidic device. Our system could easily visualize the interactions between kidney epithelial cells and ASCs. The collagen gel-encapsulated ASCs in the central channel provided a large interface to facilitate the morphological changes in epithelial cells. The cup-like structure that contains the epithelial monolayer allowed the shear stress application and fluid collection. The functional assessments also confirmed the epithelialization and maturation of the cocultured epithelium. These results, we believe, have a broad range of potential application in renal biology, such as drug screening, mechanism of kidney disease, and kidney tissue engineering.

Materials and Methods

ASC isolation and cell culture

The ASCs were harvested from the abdominal fat pad in Sprague-Dawley rats with the age of 8 weeks. The experimental design and animal protocols were reviewed and approved by the Institutional Animal Care and Use Committee (IACUC) in the National Cheng Kung University. Briefly, the subcutaneous fat pads were obtained from the abdominal fat tissue after scarification by CO_2 inhalation. The isolation of ASCs from the rat adipose tissue was modified from the previous techniques.[20] To isolate stromal cells, samples were washed extensively with phosphate-buffered saline (PBS; Invitrogen), cut into small pieces, and then digested with 0.075% collagenase (Sigma-Aldrich) at 37°C for 1 h. The collagenase was inactivated by adding an equal volume of the Dulbecco's modified Eagle's medium (DMEM; Invitrogen) with 10% fetal bovine serum (FBS; HyClone). After filtrating and lysis of red blood cells, the pelleted stromal vascular fraction was collected by the infranatant centrifuge and enriched by a plastic adherent for the preadipocyte population. The ASCs were cultured in the DMEM consisting of 10% FBS and 1% penicillin–streptomycin (Invitrogen) at 37°C in 5% CO_2. The multilineage differentiation capabilities were induced by replacing the medium to the osteogenic, chondrogenic, and adipogenic differentiation medium and verified by the methods as previously described.[20] All ASCs used in the experiments were obtained between passages 4 and 8.

MDCK (kidney epithelial cell line, ATCC, CCL34) cells were cultured in the DMEM supplemented with 10% FBS and 1% penicillin–streptomycin. Cells were cultured on a 10-cm Petri dish (Nunc) and maintained in a humidified incubator (Thermo Forma) at 37°C with 5% CO_2 as previously described.[23]

Coculture of MDCK and ASC

The coculture of MDCK and ASC in the microfluidic device was modified from the gel injection methods in polydimethylsiloxane (PDMS) microfluidics as described.[2] The photolithography master was created by spin coating a 150-μm layer of SU-8 100 negative tone photoresist material (MicroChem), followed by the processing of SU-8 fabrication steps: soft baking, exposure, postexposure baking, and development.[24] The PDMS (Sylgard 184; Dow Corning) microfluidics was made by replica casting PDMS against a master and cured at 65°C for 2 h in a vacuum chamber. As the PDMS cured, the microfluidic channels were peeled off and extensively rinsed by distilled water, and then autoclaved before the cell culture. To visualize the epithelial function, the sterilized microfluidics was assembled on a cover glass (Corning). The inlet and outlet of coculture device were connected by polyethylene tubes for injection of cells or apply fluid flow (Fig. 1A).

The coculture platform was designed with the schematic of epithelial monolayer of MDCK cells to interact with ASCs embedded in the 3D gel (Fig. 1B). The ice-cold type I collagen (rat tail; BD Bioscience) was prepared for cell culture by adding concentrated PBS (10×) and polymerized by adjusting the pH to 7.4 by using NaOH (1N; Sigma). The resuspended ASCs (1×10^6 cells/mL) were mixed with the collagen solution (1:2) to achieve an ASC-encapsulated collagen gel (CG-ASC). In groups that contain the CG only, an equal volume of PBS was mixed to maintain a similar final concentration for CG (2.5 mg/mL). Either the CG or CG-ASC were injected into the coculture device and polymerized in a humidified incubator at 37°C for 2 h. To enhance the cell attachment, the glass surface on empty channels was thin coated with type I collagen (5 μg/cm^2; BD Bioscience) for 30 min. The resuspended MDCK (1×10^7 cells/mL) were then applied to the empty chamber to form a monolayer on the cover glass. The culture environment for the assembled coculture system was kept in a regular humidified incubator for indicating time points.

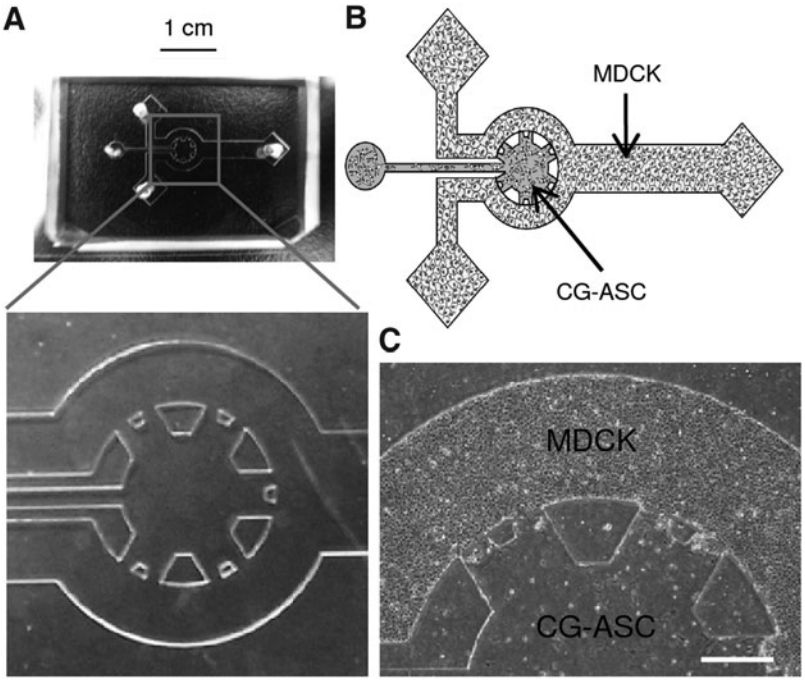

FIG. 1. The cup-like coculture system was manufactured by microfluidic technologies. Color picture of empty polydimethylsiloxane with enlarging the details of multiple channels **(A)**. Schematic diagram of microfluidic device exhibited the feature similar to the Bowman's capsule in kidney **(B)**. The adipose stem cells were embedded in the collagen gel (CG-ASC) and injected into the central channel. After polymerization of CG-ASC, the suspending kidney epithelial cells (MDCKs) were applied to the peripheral channel and formed a monolayer. A clear interface between the three-dimensional environment of CG-ASC and the epithelial monolayer of MDCKs was observed after coculture for 24 h **(C)**. The dash line shows the estimate border to confine CG-ASC by the surface tension of gel. Scale bar in **(A)** = 1 cm. Scale bar in **(C)** = 400 μm. MDCK, Madin-Darby canine kidney.

The commercial coculture transwell (BD Falcon; six-well plates) with an 8-μm pore size of polycarbonate membrane was also used to study the cell–cell interaction between MDCKs and ASCs. To compare the cellular morphology between different systems, the seeding densities for both ASCs and MDCKs in transwell are the same with these in the microfluid coculture device. The CG-ASC was polymerized in the lower compartment of a six-well plate (ASC-LC) or on the bottom of a permeable membrane (ASC-BM) by inverting the insert in a humidified incubator at 37°C for 2 h. After the gel polymerization, the insert was assembled to the transwell plate and the MDCKs were seeded in the upper compartment and formed a monolayer on the translucent permeable membrane insert. After coculture for 48 h, the MDCKs with permeable membranes were fixed and cut down from the insert for immunofluorescent staining.

Immunofluorescence staining and 3D reconstruction

To investigate the epithelium morphology, MDCKs injected into the microfluidic device were observed by both phase- and differential interference-contrast (DIC) images using a spinning disc confocal microscopy (IX-71 DSU; Olympus Co.) at 24, 48, and 72 h. Images are collected with environmental control at 37°C when acquiring the living cell confocal images. To identify the functional protein expression, the immunofluorescent staining was performed without dissembling the microfluidic device. The cells coculture in microfluidics were perfused by PBS, fixed with 4% paraformaldehyde (Sigma-Aldrich), and then permeabilized in 0.1% Triton X-100 (Sigma-Aldrich). The cell–cell junction was labeled by rabbit polyclonal beta-catenin (β-catenin) (1:200; Santa Cruz Biotech.) and followed by TRITC-conjugated secondary antibodies (1:200; Jackson ImmunoResearch Lab, Inc.). To indicate the cilia formation in epithelial cells, the fixed cells were labeled with mouse monoclonal antibodies against acetylated tubulin (Ac-Tub) (alpha tubulin, 1:200; Invitrogen), and then followed by FITC-conjugated secondary antibodies (1:200; Jackson ImmunoResearch Lab, Inc.). The function of ion transportation in the epithelial cell was labeled by an antibody against the α1 subunit of sodium/potassium-ATPase (Na^+/K^+ ATPase) (1:200; Santa Cruz Biotech.). Cell nuclei were visualized with 4,6-diamidino-2-phenylindole staining (DAPI, 1:1000; Molecular Probe, Inc.). After staining, the samples in microfluid devices were rinsed with PBS, and then mounted in a glycerol gelatin mounting medium (GG-1; Sigma-Aldrich).

Specimens were examined using a spinning disc confocal microscope that connected to a cooled-CCD camera (Olympus). The 3D image slices were acquired with 0.5-μm-thick optical sections from bottom to top of the cell in the Z-axis by using a 60x-oil objective lens, and then reconstructed by commercial software (CellR^; Olympus). The cell height of MDCKs was defined by the numbers of in-focus sections among serial 3D images for both DIC and fluorescent images. In fluorescent images, the cell height was further measured from the thickness of Z-stack images using commercial software (CellR^; Olympus). The fluorescent intensities of labeled proteins were analyzed by ImageJ Software (ImageJ). At least three areas in the peripheral channels were randomly selected and analyzed in each experiment. The number of cilia formation was counted by concentrated Ac-Tub with cilia morphology in at least three random areas for each device. All the samples for immunofluorescent staining were obtained from at least three independent experiments.

Application of fluid flow on microfluidic system

After culture the MDCKs in the microfluidic device overnight, the MDCKs were subjected to fluid shear stress in the channel. The flow was created by negative pressure of pulling the syringe (0.025 or 0.0125 mL/min) mounted on a syringe pump (NE-4000; Next-Advance Lab). The wall shear stress on the surface terminal epithelial monolayer can be

calculated by $\tau = 6Q\mu/Wh^2$, where Q is the volume flow rate, W and h are the width and height of the flow channel, and μ is the fluid viscosity.[25] The central channels containing the CG or CG-ASC were sealed by placing a PDMS block at the injection site. The fluidic path in the current device starts at the fluid reservoir, goes through injection sites and connection tubes, follows channels with cup-like features, and goes to the terminal of the collecting end before exiting the device. To avoid the complex flow pattern at the interface of the cup-like feature of the central channel, we study the living cell dynamics of MDCKs in response to the laminar shear stress, which located at the straight collecting channel. The straight part of the coculture device that contains only MDCKs has a dimension of 2 mm in width and 150 μm in height. Therefore, the estimate shear stress on MDCKs is 0.5 dyne/cm^2 with the volume of 0.025 mL/min and is 0.25 dyne/cm^2 with the volume of 0.0125 mL/min. To visualize the fluid distribution when applying flow in microfluidic channels, the PBS mixed with Trypan Blue (1:1) (Invitrogen) was used to label the liquid and immediately sucked into the channel after turning on the syringe pump. The phase-contrast images were taken at different time point by using a 10× objective lens on inverted microscopy (Olympus Co.).

Living cell observation for intracellular protein dynamics

To demonstrate the ability of monitoring protein dynamics in living cells using the current microfluidic device, the GFP-alpha-tubulin plasmid (gift of Professor Shu Chien) was transfected into MDCKs by using the Lipofectamine reagent (Invitrogen). Cells were used for coculture experiments after 36 h of transfection. After coculture of the transfected MDCKs in the microfluidic device overnight, the MDCKs were subjected to fluid shear stress as aforementioned. The GFP-tubulin was measured by a time-lapse spinning disc confocal microscope (Olympus) with an excitation wavelength of GFP at 488 nm and detected between 506 and 538 nm. The dynamics of GFP-tubulin was recorded at the speed of 1 frame/min, since 1 min before shear stress application by using a 40× objective lens. The animation of GFP-tubulin dynamics under shear stress in the coculture device was exported to the movie file by commercial software (CellR^; Olympus).

Statistics

Data represented are mean ± S.D. from three independent experiments (from different donors of rat ASCs) for each group. The differences between groups were analyzed by one-way ANOVA and the Bonferroni test for multiple comparisons, with $p < 0.05$ taken as statistically significant.

Results

Living cell monitoring for epithelial monolayer and gel-encapsulated 3D microenvironment

The microfluidic coculture system was established by embedding ASCs in the CG and a monolayer culture of MDCKs in nascent channels (Fig. 1). The ASCs were encapsulated in a 3D microenvironment by mixing them with type I CG and injecting the mixture into the central channel before crosslinking. The columnar PDMS pillars confined the CG within the central channel by surface tension and formed the 3D structure with a diameter of 3 mm and a height in 150 μm. The dimension of the central channel and distance between PDMS pillars were designed with the consideration to incorporate a high cell number of ASC, an efficient small amount of CG, and a high interaction surface with a nascent channel. As the CG polymerized, the suspending MDCKs were injected into the surrounding channels to form an epithelial monolayer (Fig. 1C).

The morphologies of the monolayer and 3D encapsulated cells were observed in phase-contrast images at 1, 24, and 48 h (Fig. 2). The suspending MDCKs were injected into the entire microfluidic channels to mimic the cell culture conditions in a commercial culture dish (Fig. 2, MDCK, left panel). At 1 h after injection, the MDCKs were attached on the glass surface and began to spread outward. The MDCK monolayer could be observed after culturing for 24 h. For the 3D gel without ASC, the CG was injected into the central channel and the suspending MDCKs were applied into the nascent channels after gel polymerization (Fig. 2, MDCK + CG, middle panel). A clear border was observed between the gel and the epithelial monolayer to demonstrate the 3D microenvironment that was created by collagen crosslinking within the central PDMS channel. The formation of the MDCK monolayer could also be observed after 24 h of culturing with the CG. At 48 h, the clear border still existed between the MDCK and the CG, thus indicating the integrity of the CG in the central channel for long-term culture. In the coculture of MDCKs with the gel-embedded ASC (CG-ASC), the application of suspending MDCKs was proceeded to the surrounding channels after the polymerization of the CG-ASC mixture (Fig. 2, MDCK + CG-ASC, right panel). The ASC embedding in the 3D CG exhibited a circular shape at 1 h after MDCK injection. After coculturing for 24 h, spindle-like morphologies were observed in the ASCs. The epithelium of the MDCK also formed at 24 h and demonstrated a clear interface between the monolayer and the 3D microenvironment after culturing for 48 h (Fig. 2, yellow arrows).

Increase of cell height and column-like epithelium by coculture system

We next measured the cell height in MDCKs after culturing for 48 h. After obtaining the phase image by using 10× objective lens, the sections in the Z-axis around the interface of the monolayer and the 3D microenvironment (Fig. 3A, yellow squares in phase images) were obtained by both DIC and fluorescent images using a confocal microscopy (Fig. 3A). The cell height was determined according to numbers of in-focus slices from serial sections in the Z-axis. By counting the number of DIC images, the cell height of MDCKs without coculture (MDCK) and cocultured with only collagen gel (MDCK + CG) were 3.44 ± 0.19 μm and 3.56 ± 0.19 μm (Fig. 3B). The MDCKs cocultured with collagen gel-embedded ASCs (MDCK + CG-ASC) increased the cell height to 5.11 ± 0.51 μm. The thickness of the cell–cell junction was visualized by immunostaining of β-catenin (Fig. 3A, IF panel) and stacking in Z sections (Fig. 3A, right panel) to confirm the cell height. The cell heights in MDCKs were quantified by measuring the thickness of Z-stack images. Only the MDCKs cultured in the microfluidic device had an average cell height of 3.5 ± 0.35 μm (Fig. 3C). The MDCKs

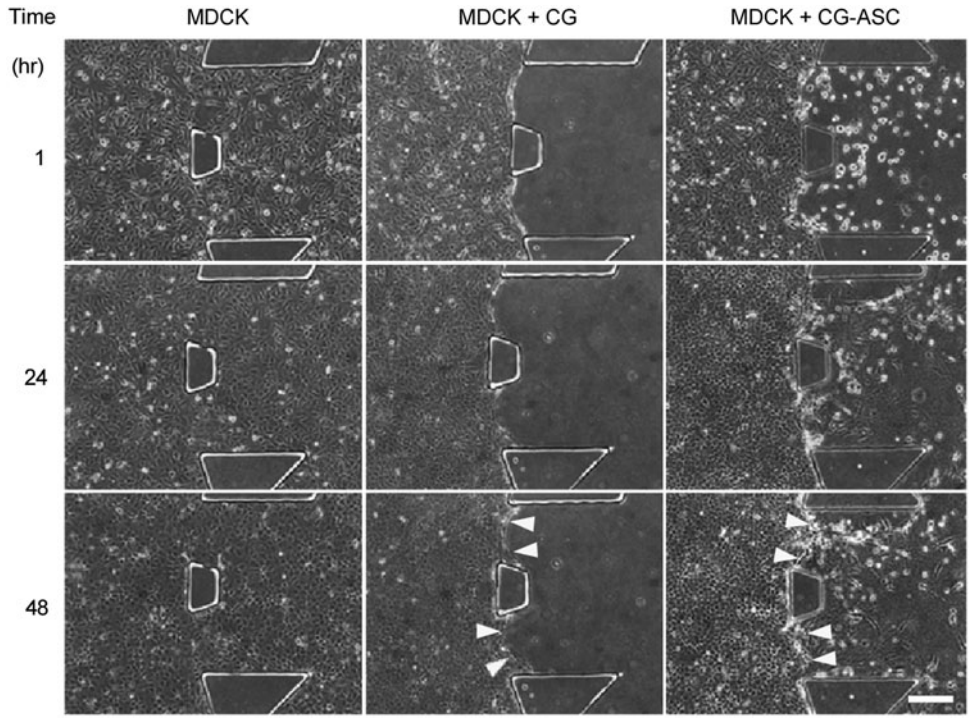

FIG. 2. Time-course images for living cells cultured in microfluidic device. The phase image of the MDCKs only (MDCK), MDCK cultured with collagen gel (MDCK + CG), or MDCKs cocultured with the ASCs encapsulating in collagen gel (MDCK + CG-ASC) were taken by 10 × objective lens after seeding for 1, 24, and 48 h. The interface between MDCKs and collagen gel (yellow arrows) still remains clear after coculture for 48 h. Scale bar = 200 μm.

cultured with the CG showed a cell height of 3.5 ± 0.1 mm, which was not taller than the cell height for culturing only MDCK. The MDCKs in the microfluidic coculture system showed a significant increase of cell height to 4.7 ± 0.37 μm with thickening of the cell–cell junction (Fig. 3C).

A commercial transwell plate was used to verify the change of cell morphology in coculture conditions. The DIC images could not distinguish the cell morphology when the MDCKs formed a monolayer on the translucent permeable membrane (Fig. 4A, DIC panel). The immunostaining of β-catenin for the MDCKs cultured on the commercial transwell membrane insert were performed after fixing the cells (Fig. 4A, IF panel). Similar to the thickening of the cell–cell junction as demonstrated in the microfluidic device, an increase of cell height was found in the MDCKs when cocultured with CG-ASC both in the lower compartment of a six-well plate (ASC-LC) and on the bottom of the permeable membrane (ASC-BM) (Fig. 4A, Z-stack panel). The quantified thickness of the cell–cell junction demonstrated that either coculturing the CG-ASC in the lower compartment or on the bottom of the membrane facilitated the columnar shape in MDCKs (Fig. 4B). This suggested that the increase of cell height in cocultured MDCKs may be through direct cell–cell contact (ASC-BM) or through the paracrine effect (ASC-LC) that release some factors to the upper compartment of the transwell insert. However, the commercial transwell plate limited the ability of living cell observation when performing the coculture experiments.

Inducing epithelial function and cilia formation in cocultured MDCKs

We tested the functional expression pattern of ion transportation in the kidney epithelium, which is essential for urine formation. The Na^+/K^+ ATPase form a complex (by alpha and beta subunits) on the cell membrane that couples the hydrolyzed ATP to import three Na^+ ions and two K^+ ions against their respective electrochemical gradients.[26] When culturing the MDCKs in the microenvironment containing the collagen gel (both in CG and CG-ASC conditions), the Na^+/K^+ ATPase showed increases on the cell membrane by labeling with the fluorescent intensity for the antibody against the α1 subunit of Na^+/K^+ ATPase (Fig. 5A). The quantification of fluorescent intensity further confirmed the induction of iron channel proteins (Fig. 5C). This indicates that culturing the MDCK in the microenvironment containing the CG could enhance the expression of Na^+/K^+ ATPase. The encapsulation of ASCs in the 3D gel can further increase this protein expression in cocultured MDCKs ($p < 0.05$, between MDCK + CG and MDCK + CG-ASC) (Fig. 5C).

The functional epithelial cells have primary cilia on the apical surface of the lumen.[27] Cilia can be visualized using immunofluorescence microscopy and primary antibodies to mark the axoneme and adjacent basal body. Acetylation of tubulin results in stabilization of tubulin polymers during mitosis. In quiescent epithelial cells, the Ac-Tub is strongly enriched in microtubules to form the cilia. For culturing only MDCKs, the tubulin was widely distributed within cytosol, barely revealing the concentrated Ac-Tub (yellow arrows) to form the cilia (Fig. 5B). The MDCK culture with CG did not increase the cilia formation, either. However, the accumulations of Ac-Tub were observed in MDCK when coculturing in the CG-ASC microfluidic system for 48 h (Fig. 5B). The quantified results showed a significant induction of cilia formation with the number of 329.8 ± 28.6 per mm^2 in cocultured MDCKs (Fig. 5D). These results indicated the beneficial effects in MDCKs by creating a culture environment in a microfluidic device using the CG and further enhancing functional epithelialization by coculturing with ASCs.

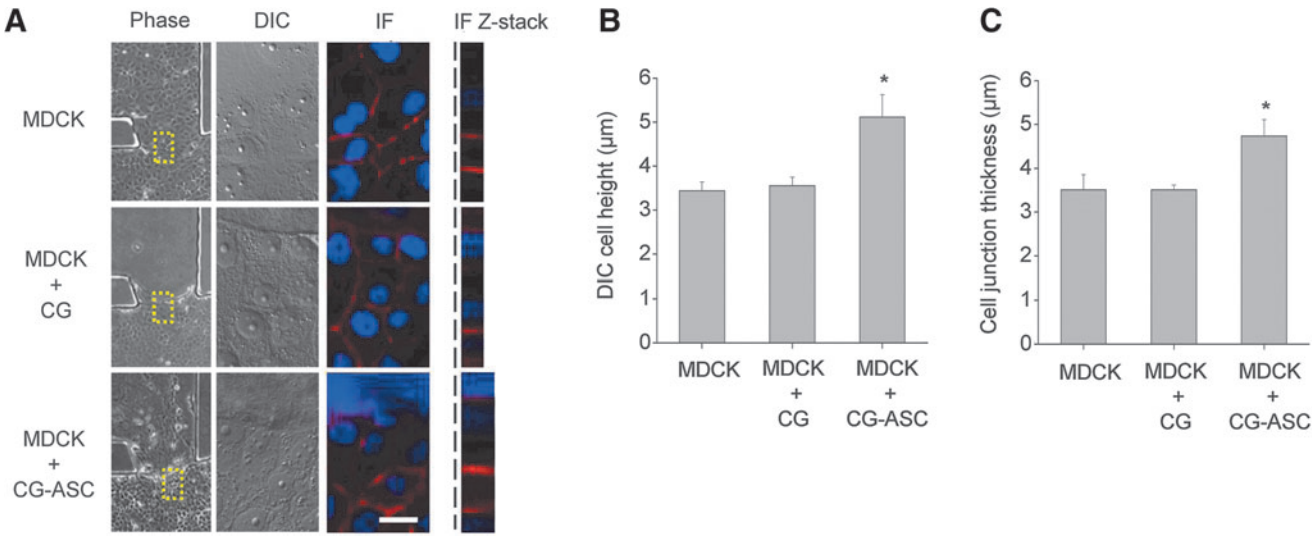

FIG. 3. Coculturing the MDCK with CG-ASC enhanced columnar morphogenesis. The cell height was investigated in MDCKs (dotted lines) after cultured with different conditions for 48 hours. A taller cell height was measured from the increased number of in-focus Z-sections using differential interference contrast (DIC) images in a spinning disc confocal microscopy. The immunofluorescent staining (IF) of β-catenin was also used to demonstrate the thickening of cell–cell junction in MDCKs when coculturing with CG-ASC by measuring the stacks of Z-sections **(A)**. Increasing the number of in-focus DIC images indicated the significant increase of cell height in cocultured MDCKs **(B)**. The quantitative analysis in the thickness of cell junction was measured from Z-stack images **(C)**. Scale bar = 20 μm. *Significant difference ($p < 0.05$) from culture only MDCKs.

Applying fluid flow to MDCKs in coculture device

The capability of observing the dynamic intracellular responses in MDCKs with the application of fluid flow is also an advantage of the current coculture microfluidic platform. The GFP-alpha-tubulin plasmid was transfected into MDCKs for acquiring the dyanmics of tubulin under fluid flow. After assembling the microfluidic device and polymerizing the CG-ASC in the central channel, the transfected MDCKs were applied into the nascent channels and incubated overnight to form a monolayer. The fluid flow was applied to the MDCKs by pumping the culture medium using a syringe pump. The straight part of the terminal collecting channel cultured with MDCK has the dimension of 0.2 cm in width and 150 μm in

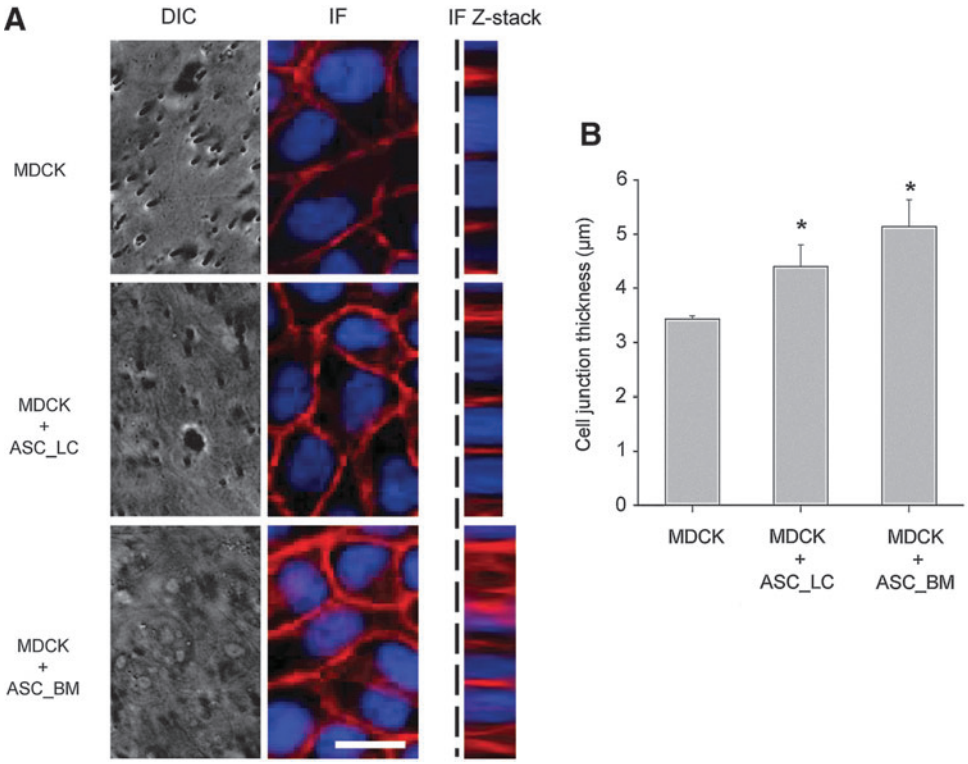

FIG. 4. Morphological verifications by commercial transwell system. The MDCKs monolayers were formed on the upper surface of the permeable membrane insert. The CG-ASC was polymerized in the lower compartment of a six-well plate (ASC-LC) or on the bottom of the permeable membrane (ASC-BM) **(A)**. However, the commercial transwell cannot observe the cell morphology when acquiring the DIC images. The quantitative analysis for measuring the thickness of cell junction can only be performed in fixed cells from Z-stack images after immunostaining **(B)**. The thickening of cell–cell junction in MDCKs was confirmed by immunofluorescent staining of β-catenin when coculture in both ASC-LC and ASC-BM conditions. *Significant difference ($p < 0.05$) from culture only MDCKs.

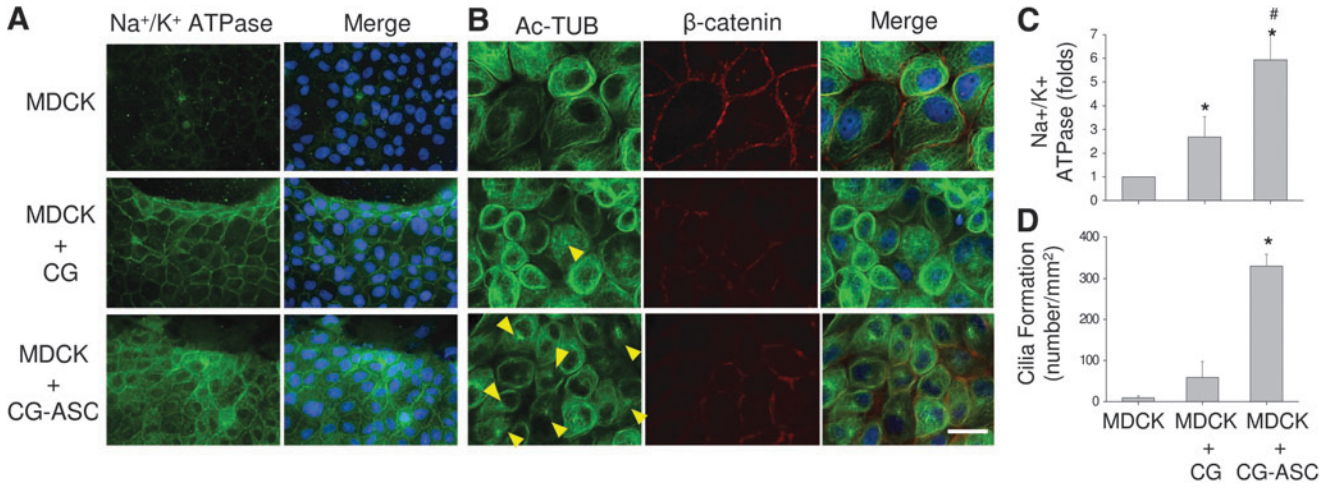

FIG. 5. Coculture system promoted the expression of functional markers in MDCKs. The fluorescent intensity of α1 subunit of Na^+/K^+ ATPase was increased in MDCKs when applying collagen gel (both of CG and CG-ASC groups) **(A)**. The concentrated acetylated tubulin (Ac-TUB, yellow arrows) indicated the induction of cilia formation in the MDCKs after cocultured with the CG-ASC for 48 h **(B)**. Significant increases of Na^+/K^+ ATPase intensity **(C)** and cilia numbers **(D)** demonstrated the functionalization of epithelial monolayer in the current microfluidic device. Scale bar = 50 μm. *Significant difference ($p < 0.05$) from culture only MDCKs. #Significant difference ($p < 0.05$) between MDCK + CG and MDCK + CG-ASC.

height. As the calculation mentioned in methodology, the shear stress was estimated about 0.5 dyne/cm^2 with pulling of the liquid at 0.025 mL/min and about 0.25 dyne/cm^2 with 0.0125 mL/min of pump speed. When coculture the transfected MDCKs with CG-ASC under static condition (time = 0), the GFP-tubulin also showed a concentrated spot near the cell nucleus (Fig. 6A). The distribution pattern of tubulin was similar to the cilia formation that labeled by using the Ac-Tub antibody in Figure 5B. With the application of shear stress at 0.5 dyne/cm^2, the changes of GFP expression and distribution indicated the dynamics of microtubules in response to fluid flow using the current coculture device (Supplementary Movie S1; Supplementary Data are available online at www.liebertpub.com/tea). Since the MDCKs formed a monolayer in coculture with CG-ASC, the cell migration and morphology under shear stress did not show

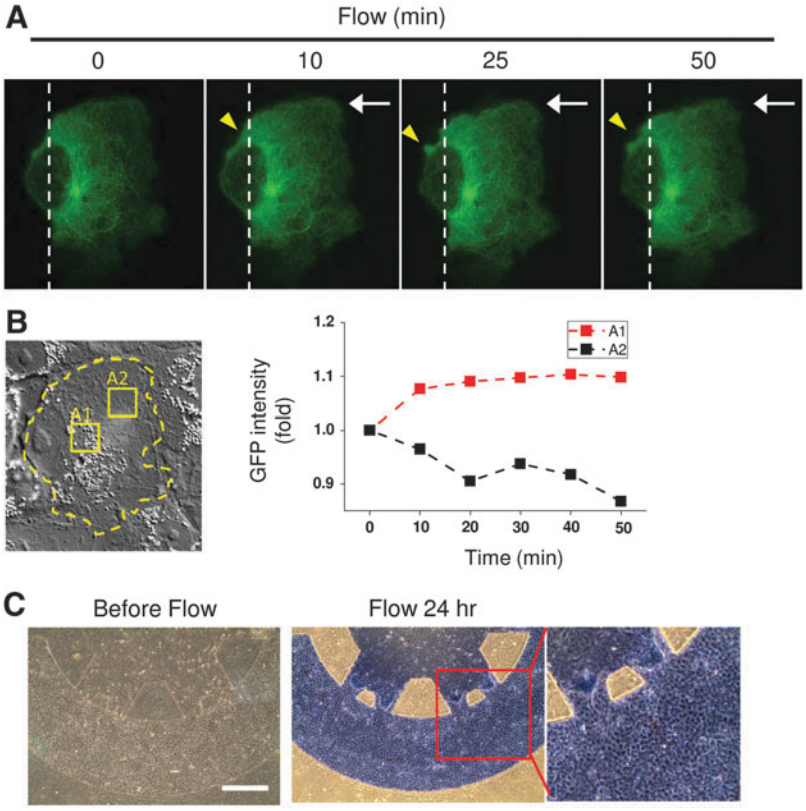

FIG. 6. Fluid shear stress was applied to the MDCKs in the cocultured microfluidic device by negative pressure of pulling the syringe pump. The flow rate was created by culture medium flow using a pumping syringe and set at 0.025 mL/min to create an estimate shear stress of 0.5 dyne/cm^2 on MDCKs. The dynamics of alpha tubulin was visualized by transfection of GFP-tubulin plasmid into the MDCKs and taking the time-lapse images by confocal microscopy when subjecting to the shear stress with the direction from right to left (white arrows) **(A)**. The phase image showed a confluence monolayer of coculture MDCK with labeling of the cell border (yellow dash line) before the application of shear stress [time 0 in **(A)**] **(B)**. Increases of GFP-tubulin near the cell nucleus (A1 area) were observed with quantifying the GFP intensities of other intracellular areas (A2 area) after shear stress application. The shear stress also increased the membrane protrusion [yellow arrows in **(A)**]. The structure of coculture environment still maintains properly after applying fluid flow at 0.25 dyne/cm^2 for 24 h **(C)**. Both MDCKs and ASCs were still alive by negative staining of Trypan Blue, which suggested the success of the proposed microfluidic device with novelties in coculture and fluid exchange. Scale bar = 400 μm.

a significant change as compared to the refer position (white dash line in Fig. 6A). The cell boundary of transfected MDCK was labeled with a yellow dash line in the phase image before the application of shear stress (time = 0) (Fig. 6B). When normalizing the GFP intensities to the same areas before shear stress, the quantification in the area A1 and A2 showed different spatial distributions. The GFP-tubulin expression was increased at the area near the nucleus (A1 area) as well as at the cell periphery with downstream of shear stress (yellow arrow) (Fig. 6B).

We hope the proposed microfluidic device can be integrated into hemodialysis systems in the future. Thus, the applying of fluid flow and testing the integrity of the device under shear stress is essential for coculture microenvironments. The coculture device was created by seeding different cells using a cell culture medium and incubated overnight to allow the cell to spread out. The coculture conditions of ASCs in the 3D CG and monolayer of MDCKs were assessed with long-term application of fluid flow. After 24 h of shear stress application, the PBS mixed with Trypan Blue was applied into the microfluidic channel by using a syringe pump. The coculture microenvironment still showed a clear border between the CG-ASC and the MDCK channels after applying flow for 24 h (Fig. 6C). The cells were still viable and excluded the Trypan Blue from staining. This proved the possibility to provide fluid exchange in current microfluidic devices without damaging the coculture structure or cells.

Discussion

The design of the current coculture microfluidic device is inspired by the naturally anatomical structure of the Bowman's capsule in the human kidney. The Bowman's capsule inside the nephron has a cup-like sac at the beginning of the tubular component to perform the first filtration of blood to form urine. There are two poles for the capsule: the vascular pole contains arterioles and encloses a glomerulus in the sac; and the urinary pole is the side with the proximal convoluted tubule. The network of glomerulus in the capsule provides a vast 3D surface area on the fenestrated vessels with a high filtration rate via ultrafiltration and collects the fluid efficiently by the surrounding proximal tubule. In the current study, the central channel was not culturing the endothelial cells nor was it responsible for fluid filtration. However, the cup-like platform provided a wide interface for epithelial cells to interact with the CG-ASC. The CG-ASC can be easily injected into the central channel with small amounts of both the CG and ASCs. The fluid was collected at the terminal of a cup-like channel. By current feature, the coculture environment can be seen as a single capsule unit for studying the cell–cell interactions.

The fluid flow in the current study was chosen at 0.25 or 0.5 dyne/cm^2 according to the study to trigger the mechanosensation in kidney tubular epithelial cells.[28] The fluid flow has some beneficial effects on epithelial cells. Application of shear stress at 1 dyne/cm^2 in primary cultured inner medullary collecting duct cells from the rat kidney facilitated the translocation of aquaporin-2, vasopressin-regulated water channel protein, to the apical surface.[29] The shear stress of the renal collecting duct in rat is depending on the rate of urine production and estimated in a range of 0.2–20 dyne/cm^2.[30] The microfluidic device designed in the current study is able to cover the range of possible shear stress in the collecting duct for relative *in vitro* study in the future. For the commercial hemodialysis system in a clinic, the dialysis machine usually sets the blood flow rates at 400 mL/min and the dialysate flow rates between 350 and 800 mL/min.[31] Since we only applied the fluid flow rate at 0.025 mL/min in a single microfluidic device and at least in the order of 10^5 flow rates should increase to provide sufficient fluid exchange if willing to connect the current device with the dialysis machine, the collection of fluid from multiple units of current microfluidic design is necessary for future hemodialysis. By distributive multiple branching of the microfluidic channels, the amplification of the coculture units to array-like chips could be achieved and allowed to inject/collect fluid simultaneously. Running multiple units of the current device in parallel could increase the volume of fluid passing through the coculture environment and collect sufficient media that contain enough factors released by cocultured cells to treat the kidney diseases.

Utilizing the principles of tissue engineering, 3D growth of cells on polymeric scaffolds provides a more physiologic condition to induce cell differentiation and tissue reconstruction.[32,33] Furthermore, the 3D structure exhibited physiological microenvironments superior to the 2D surfaces in cell morphology, adhesion, proliferation, and migration.[34,35] The coculture system manufactured by BioMEMS technologies have the specialty to create dynamic cell–cell interactions for liver tissue[36] or reconstitute organ-level lung functions with mechanical stretch.[37] The culture of MDCK in microfluidic device with application of shear stress was performed to study the force transduction mechanism in promoting cell polarization,[38] cytoskeletal reorganization,[38,39] and intracellular Ca^{2+} response.[39] Different from previous studies that only seeded MDCK in microfluidic device, the current coculture device discovered the MDCK formed a monolayer and changed the morphology when interacting with the 3D CG-ASC. One of the advantages in the current design is, easy to separate two cell populations by capsuling ASC in the 3D CG, and then apply the MDCK to form a monolayer. A coculture of two cell types with specific geometry in 2D circumstance may also be achieved by micropatterning a different ECM for desired cells with multiple surface coating and cell-seeding procedures. A specific geometry of ECM coating is difficult to perform in the microfluidic device. Furthermore, both ASCs and MDCKs are using collagen as the ECM for cell adhesion in the current study. Even coculture of ASCs and MDCKs could be achieved in 2D circumstance; the application of fluid shear stress only to MDCKs is also a difficult task. This microfluidic device can immediately observe the phenotypic changes and further provide insights into the underlying mechanisms of cell–cell interactions in both types of cells. Since we can apply fluid flow to this coculture microenvironment, the cell–cell interaction and functional remodeling in renal biology under shear stress can be studied using the current device.

Another advantage for the current coculture platform involves the use of ASCs. The transplantation of embryonic stem cells (ESCs) may also provide similar results. However, usage of ESCs raised great ethical concerns and consequential teratoma formations. Once the ESCs are transplanted into the host, the immunosuppressant agents are indispensable. Unlike ESCs or other precursor cells, several advantages in

ASCs promote clinical application potentials, which include the following: (1) abundant in quantities that can be acquired; (2) ease in harvesting under minimally invasive procedures; and (3) autologous origins that are ready for further clinical application.[40] Udo *et al.* embedded adipose tissue fragments in a 3D CG and developed an organotypic culture by overlaying a monolayer of MDCKs.[18] Promotion of the structural differentiation in MDCKs was found in coculturing with ASCs isolated from subcutaneous or perirenal adipose tissues, but not in coculturing with 3T3 fibroblasts. The mechanism for the adipose tissue to promote the hypertrophy, polarization, and differentiation of MDCKs were determined by opposing the endocrine or paracrine effects of leptin and adiponectin to attenuate the growth and apoptosis of MDCKs.[18] We also observed the polarization and maturation of MDCKs in the current microfluidic device. The coculture of CG-ASC in the lower compartment and MDCKs in the upper transwell insert also facilitated the columnar shape in MDCKs by using the commercial transwell system in this study. These suggested the paracrine effects for ASCs to interact with MDCKs when embedded in the 3D CG. When applying the Trypan Blue into the coculture system, the negative staining demonstrated high viability in MDCKs with subjected to fluid flow. To focus on the beneficial effect of MDCK functionalization using current coculture microfluidic device, we did not address the responses of ASCs embedded in the CG and cocultured with MDCKs. These are very interesting and important issues, which could be studied by using the current platform. Besides, autologous adult stem cells are the most ideal source for clinical application in regenerative medicine. Other sources of stem/precursor cells, such as MSCs,[41] placenta-derived multipotent cells,[25] or kidney progenitor cells[42] may also be applied into the CG to explore the applications.

Columnar morphogenesis was observed in cocultured MDCKs. The epithelium in the kidney tissue is asymmetric or polarized with cells in columnar shape.[43] Lateral membranes provide cell–cell adhesion and diffusion barriers, which are possessed by desmosomes, adheren junctions, and tight junctions. The microtubule plays an important role in the morphogenesis of columnar-shaped and polarized epithelial cells.[44] Cilia formation also demonstrated the functional epithelialization in MDCKs. Although the detail function of cilia on the kidney epithelium is still unknown, a defect of the primary cilium in the renal tube cells can lead to polycystic kidney disease.[45–47] The Na-K-ATPase, also known as the sodium pump, is involved in the formation of tight junctions and regulation of intracellular sodium homeostasis.[48] The normal function of Na-K-ATPase in the tight junction assembly is related to RhoA GTPase and stress fibers in epithelial cells. Loss of polarity and mislocalization of Na-K-ATPase is also related to polycystic kidney disease. Taken together, our results in increased cell height, cilia formation, and Na-K-ATPase expression demonstrated the improvement of the epithelial function in MDCKs by coculturing with CG-ASC in the microfluidic device. Other functional assessments may also be incorporated to verify the clearance of creatinine (Cr) or leakages of urea nitrogen (UN) by seeding the epithelial cells on the porous membrane.[10] UN and Cr were added at concentrations of 20 mM UN and 5.0 mg/dL Cr to the basal medium after the cells reached a confluence and formed a monolayer. In the current study, the monolayer of MDCKs was seeded on the cover glass and unable to test the permeability of the epithelium. However, the clearance rate of different wastes may still be evaluated with various flow rates and culture conditions in the future.

Other hydrogels, such as Matrigel and agarose, may also be incorporated to current microfluidic devices. The 3D gel must encapsulate the ASC and not damage those cells during polymerization processes. Thus, ultraviolet photo-polymerization using PEG derivatives[7] or ionic crosslinking of alginate[49] are not appropriate for the current platform. A multilayer structure for a 3D coculture by using layer-by-layer microfluidic technology may also achieve results similar to the current platform. The multilayer design may prevent the diffusion of fluid from the epithelial channel to the CG during the application of fluid flow. However, the usage of a porous membrane to create a multilayer could prohibit the direct cell–cell contact and living cell observations. Although the current platform demonstrated several benefits for coculture of the MDCK and ASC, there are some improvements that need to be done in the future. First, the dimensions of channel are not optimized during design and layout. There are several factors that need to be considered when designing the central and peripheral channels, such as a large cell–cell interaction surface, efficient amount of ASC and CG to stimulate MDCK functionalization, flow pattern and application methods in the MDCK channel. These parameters are currently optimizing computational simulation and testing the responses in both types of cells for future biomedical applications.

Conclusion

The schematic diagram of the current microfluidic device provides ASCs embedded in the CG and directly interact with MDCKs. The cup-like peripheral channel allows the MDCKs to have a large interface with the central channel that contains CG-ASC. Coculturing with GC-ASC enhanced cilia formation and renal epithelial functions in MDCKs. The current coculture platform can apply shear stress on epithelial cells and allow fluid exchange. These advantages may provide beneficial innovations for developing renal chips in the future.

Acknowledgments

The authors are thankful for the usage of facilities at the Center for Micro/Nano Science and Technology facilities (CMNST) in NCKU to microfabricate the microfluidic devices. We are also thankful for the plasmid gift and supports from Professor Shu Chien in UC San Diego. This work was supported, in part, by National Science Council (Taiwan) Grants NSC 99-2320-B-006-002-MY3, NSC 98-2627-B-006-010-MY3, and NSC 97-2314-B-006-063- MY2, and, in part, from the National Health Research Institute (Taiwan) by Grant NHRI- EX101-10115EC.

Disclosure Statement

No competing financial interests exist.

References

1. Whitesides, G.M. What comes next? Lab Chip **11,** 191, 2011.

2. Chung, S., Sudo, R., Mack, P.J., Wan, C.R., Vickerman, V., and Kamm, R.D. Cell migration into scaffolds under co-culture conditions in a microfluidic platform. Lab Chip **9,** 269, 2009.
3. Lii, J., Hsu, W.J., Parsa, H., Das, A., Rouse, R., and Sia, S.K. Real-time microfluidic system for studying mammalian cells in 3D microenvironments. Anal Chem **80,** 3640, 2008.
4. Bhatia, S.N., Balis, U.J., Yarmush, M.L., and Toner, M. Effect of cell-cell interactions in preservation of cellular phenotype: cocultivation of hepatocytes and nonparenchymal cells. FASEB J **13,** 1883, 1999.
5. Khetani, S.R., and Bhatia, S.N. Microscale culture of human liver cells for drug development. Nat Biotechnol **26,** 120, 2008.
6. Patel, S., Thakar, R.G., Wong, J., McLeod, S.D., and Li, S. Control of cell adhesion on poly(methyl methacrylate). Biomaterials **27,** 2890, 2006.
7. Albrecht, D.R., Tsang, V.L., Sah, R.L., and Bhatia, S.N. Photo- and electropatterning of hydrogel-encapsulated living cell arrays. Lab Chip **5,** 111, 2005.
8. Huh, D., Torisawa, Y.S., Hamilton, G.A., Kim, H.J., and Ingber, D.E. Microengineered physiological biomimicry: organs-on-chips. Lab Chip **12,** 2156, 2012.
9. Snouber, L.C., Letourneur, F., Chafey, P., Broussard, C., Monge, M., Legallais, C., *et al.* Analysis of transcriptomic and proteomic profiles demonstrates improved Madin-Darby canine kidney cell function in a renal microfluidic biochip. Biotechnol Prog **28,** 474, 2012.
10. Saito, A., Sawada, K., and Fujimura, S. Present status and future perspectives on the development of bioartificial kidneys for the treatment of acute and chronic renal failure patients. Hemodial Int **15,** 183, 2011.
11. Humes, H.D., MacKay, S.M., Funke, A.J., and Buffington, D.A. Tissue engineering of a bioartificial renal tubule assist device: *in vitro* transport and metabolic characteristics. Kidney Int **55,** 2502, 1999.
12. Asano, M., Fujita, Y., Ueda, Y., Suzuki, D., Miyata, T., Sakai, H., *et al.* Renal proximal tubular metabolism of protein-linked pentosidine, an advanced glycation end product. Nephron **91,** 688, 2002.
13. Humes, H.D., Buffington, D.A., MacKay, S.M., Funke, A.J., and Weitzel, W.F. Replacement of renal function in uremic animals with a tissue-engineered kidney. Nat Biotechnol **17,** 451, 1999.
14. Su, H.W., Wang, S.W., Ghishan, F.K., Kiela, P.R., and Tang, M.J. Cell confluency-induced Stat3 activation regulates NHE3 expression by recruiting Sp1 and Sp3 to the proximal NHE3 promoter region during epithelial dome formation. Am J Physiol Cell Physiol **296,** C13, 2009.
15. Jiang, S.T., Liao, K.K., Liao, M.C., and Tang, M.J. Age effect of type I collagen on morphogenesis of Mardin-Darby canine kidney cells. Kidney Int **57,** 1539, 2000.
16. Wu, M.J., Wen, M.C., Chiu, Y.T., Chiou, Y.Y., Shu, K.H., and Tang, M.J. Rapamycin attenuates unilateral ureteral obstruction-induced renal fibrosis. Kidney Int **69,** 2029, 2006.
17. Axelsson, J., and Stenvinkel, P. Role of fat mass and adipokines in chronic kidney disease. Curr Opin Nephrol Hypertens **17,** 25, 2008.
18. Udo, K., Aoki, S., Uchihashi, K., Kawasaki, M., Matsunobu, A., Tokuda, Y., *et al.* Adipose tissue explants and MDCK cells reciprocally regulate their morphogenesis in coculture. Kidney Int **78,** 60, 2010.
19. Zuk, P.A., Zhu, M., Ashjian, P., De Ugarte, D.A., Huang, J.I., Mizuno, H., *et al.* Human adipose tissue is a source of multipotent stem cells. Mol Biol Cell **13,** 4279, 2002.
20. Zuk, P.A., Zhu, M., Mizuno, H., Huang, J., Futrell, J.W., Katz, A.J., *et al.* Multilineage cells from human adipose tissue: implications for cell-based therapies. Tissue Eng **7,** 211, 2001.
21. Liu, T.M., Martina, M., Hutmacher, D.W., Hui, J.H., Lee, E.H., and Lim, B. Identification of common pathways mediating differentiation of bone marrow- and adipose tissue-derived human mesenchymal stem cells into three mesenchymal lineages. Stem Cells **25,** 750, 2007.
22. Yoshimura, H., Muneta, T., Nimura, A., Yokoyama, A., Koga, H., and Sekiya, I. Comparison of rat mesenchymal stem cells derived from bone marrow, synovium, periosteum, adipose tissue, and muscle. Cell Tissue Res **327,** 449, 2007.
23. Wu, C.C., Su, H.W., Lee, C.C., Tang, M.J., and Su, F.C. Quantitative measurement of changes in adhesion force involving focal adhesion kinase during cell attachment, spread, and migration. Biochem Biophys Res Commun **329,** 256, 2005.
24. Wu, C.C., Li, Y.S., Haga, J.H., Kaunas, R., Chiu, J.J., Su, F.C., *et al.* Directional shear flow and Rho activation prevent the endothelial cell apoptosis induced by micropatterned anisotropic geometry. Proc Natl Acad Sci U S A **104,** 1254, 2007.
25. Wu, C.C., Chao, Y.C., Chen, C.N., Chien, S., Chen, Y.C., Chien, C.C., *et al.* Synergism of biochemical and mechanical stimuli in the differentiation of human placenta-derived multipotent cells into endothelial cells. J Biomech **41,** 813, 2008.
26. Gadsby, D.C. Ion channels versus ion pumps: the principal difference, in principle. Nat Rev Mol Cell Biol **10,** 344, 2009.
27. Satir, P., and Christensen, S.T. Structure and function of mammalian cilia. Histochem Cell Biol **129,** 687, 2008.
28. Zhou, J. Polycystins and primary cilia: primers for cell cycle progression. Annu Rev Physiol **71,** 83, 2009.
29. Jang, K.J., Cho, H.S., Kang do, H., Bae, W.G., Kwon, T.H., and Suh, K.Y. Fluid-shear-stress-induced translocation of aquaporin-2 and reorganization of actin cytoskeleton in renal tubular epithelial cells. Integr Biol **3,** 134, 2011.
30. Cai, Z., Xin, J., Pollock, D.M., and Pollock, J.S. Shear stress-mediated NO production in inner medullary collecting duct cells. Am J Physiolo Renal Physiol **279,** F270, 2000.
31. Bhimani, J.P., Ouseph, R., and Ward, R.A. Effect of increasing dialysate flow rate on diffusive mass transfer of urea, phosphate and beta2-microglobulin during clinical haemodialysis. Nephrol Dial Transplant **25,** 3990, 2010.
32. Desoize, B. Contribution of three-dimensional culture to cancer research. Crit Rev Oncol Hematol **36,** 59, 2000.
33. Takezawa, T. A strategy for the development of tissue engineering scaffolds that regulate cell behavior. Biomaterials **24,** 2267, 2003.
34. Griffith, L.G., and Swartz, M.A. Capturing complex 3D tissue physiology *in vitro*. Nat Rev Mol Cell Biol **7,** 211, 2006.
35. Raines, E.W. The extracellular matrix can regulate vascular cell migration, proliferation, and survival: relationships to vascular disease. Int J Exp Pathol **81,** 173, 2000.
36. Hui, E.E., and Bhatia, S.N. Micromechanical control of cell-cell interactions. Proc Natl Acad Sci U S A **104,** 5722, 2007.
37. Huh, D., Matthews, B.D., Mammoto, A., Montoya-Zavala, M., Hsin, H.Y., and Ingber, D.E. Reconstituting organ-level lung functions on a chip. Science **328,** 1662, 2010.
38. Jang, K.J., and Suh, K.Y. A multi-layer microfluidic device for efficient culture and analysis of renal tubular cells. Lab Chip **10,** 36, 2010.

39. Wang, J., Heo, J., and Hua, S.Z. Spatially resolved shear distribution in microfluidic chip for studying force transduction mechanisms in cells. Lab Chip **10,** 235, 2010.
40. Gimble, J.M., Katz, A.J., and Bunnell, B.A. Adipose-derived stem cells for regenerative medicine. Circ Res **100,** 1249, 2007.
41. Pittenger, M.F., Mackay, A.M., Beck, S.C., Jaiswal, R.K., Douglas, R., Mosca, J.D., *et al.* Multilineage potential of adult human mesenchymal stem cells. Science **284,** 143, 1999.
42. Lee, P.T., Lin, H.H., Jiang, S.T., Lu, P.J., Chou, K.J., Fang, H.C., *et al.* Mouse kidney progenitor cells accelerate renal regeneration and prolong survival after ischemic injury. Stem Cells **28,** 573, 2010.
43. Bryant, D.M., and Mostov, K.E. From cells to organs: building polarized tissue. Nat Rev Mol Cell Biol **9,** 887, 2008.
44. Musch, A. Microtubule organization and function in epithelial cells. Traffic **5,** 1, 2004.
45. Gray, M.A. Primary cilia and regulation of renal Na+ transport. Focus on "Heightened epithelial Na+ channel-mediated Na+ absorption in a murine polycystic kidney disease model epithelium lacking apical monocilia". Am J Physiol Cell Physiol **290,** C947, 2006.
46. Siroky, B.J., Ferguson, W.B., Fuson, A.L., Xie, Y., Fintha, A., Komlosi, P., *et al.* Loss of primary cilia results in deregulated and unabated apical calcium entry in ARPKD collecting duct cells. Am J Physiol Renal Physiol **290,** F1320, 2006.
47. Ong, A.C., and Wheatley, D.N. Polycystic kidney disease—the ciliary connection. Lancet **361,** 774, 2003.
48. Rajasekaran, A.K., and Rajasekaran, S.A. Role of Na-K-ATPase in the assembly of tight junctions. Am J Physiol Renal Physiol **285,** F388, 2003.
49. Braschler, T., Johann, R., Heule, M., Metref, L., and Renaud, P. Gentle cell trapping and release on a microfluidic chip by *in situ* alginate hydrogel formation. Lab Chip **5,** 553, 2005.

Address correspondence to:
Chia-Ching Wu, PhD
Department of Cell Biology and Anatomy
National Cheng Kung University
Tainan 701
Taiwan

E-mail: joshccwu@mail.ncku.edu.tw

Received: October 9, 2012
Accepted: April 1, 2013
Online Publication Date: July 2, 2013